Design of Wireless Power Transmission Coupling Structure Based on Rotary Steerable Drilling

Li Ji, Fuchen Ge, and Chi Zhang

***Abstract*—In this article, a DD-4D double-layer orthogonal magnetic coupler with mutual inductance compensation is proposed for powering electrical equipment mounted on fixed sleeve during rotary steerable drilling. It can not only transfer the electric energy from the rotating side to the stationary side, but also ensure the stability of the transmission efficiency of the wireless power transmission system. First, the topology and working principle of DD-4D double-layer orthogonal coils are proposed and the typical WPT system of rotary steerable drilling is analyzed. Second, the influence of the center angle and the number of combinations of DD transmitting coils with good lateral antimigration performance on mutual inductance of the magnetic coupler was investigated. Third, the DD-4D double-layer orthogonal coils' model is determined to solve the problem of mutual inductance zero coupling point during rotation. Fourth, the simulation characteristics of lateral migration axial migration and off-axis angular migration are studied, respectively. Fifth, an experimental model is established to verify that the comprehensive efficiency of the system is 88.56% and the efficiency offset rate is only 3.34%.**

***Index Terms*—Magnetic coupler, mutual inductance compensation, rotary wireless energy transmission, uniform magnetic field.**

I. Introduction

Oil and gas, as the most important primary energy of human society, have an important impact on social stability and prosperity. With the continuous advancement of downhole development, well depth gradually increases and the environment becomes more and more complex [1], [2], [3]. The power supply of deep-well drilling equipment is usually provided by turbine generator driven by high-pressure mud in drill pipe [4]. In the drilling process, the reliability of electric energy transmission is challenged by harsh conditions such as high temperature, high pressure, vibration, and liquid convection [5], [6], [7], [8], [9].

The traditional wired connection mode is not suitable for energy and signal transmission under drilling conditions, while the brush slip ring mode has the problem of seal failure in the well. The wireless energy transmission technology based on the principle of electromagnetic resonance can realize power transmission under the condition of complete electrical isolation [10], [11], without the problem of contact fire and seal failure. It can effectively reduce equipment wear and improve transmission reliability.

In the mechanical structure of rotary steerable drilling system, there is relative rotation between the rotary drill pipe and the fixed guide sleeve. How to conduct wireless power transmission for the static working equipment through the rotary generating device is an important research topic in this field [12], [13]. Coupling coils are the core component of wireless power transmission system, and the change of its parameters can affect the change of space magnetic field, and ultimately affect the transmission efficiency and robustness of the system [14], [15], [16], [17], [18].

In order to better adapt to the rotation condition, the coupling coils are often circular. The model in which the transmitting and receiving coils are all round is called fully wrapped model. Song et al. [19], at Harbin Institute of Technology, proposed a SCSC-Type magnetic coupling coils, which ensures the stability of efficiency and lightweight structure, but has a low degree of integration. Abdolkhani et al. [20] compared and analyzed the transmission performance of the inner and outer coils and the parallel coils under rotating conditions, and on this basis proposed a parallel coils with primary side-secondary side-primary structure, which could increase the power by four times compared with the typical double coils model. Based on the periodicity of the rotation of the equipment, the utilization rate of the wire can be improved by replacing the whole circle with an arc, or by appropriately reducing the size of one side coil. This kind of structure is called semiencircle structure. Wang et al. [21] proposed a radial flux rotating wireless power transmission system, which adopted the DD-DD magnetic coupler, where in the central angle of the unilateral receiving coils was only 60°, which reduced the coils winding amount. However, the model had zero coupling point of mutual inductance in the rotation process, which affected the stability of transmission efficiency. In [22], two solenoid coils with a difference of 120° between their central angles were used on the transmitting side to improve the utilization rate of wires. Meanwhile, internal and external overlapping was adopted on the receiving side to compensate for mutual inductance of coils, reducing the migration rate of mutual inductance in the rotation process. Abdolkhani et al. [23] proposed the model of multiple transmitting coils, with six T-shaped ferrites corresponding to the solenoid coils one by one, and the receiving coils wound on the shaft. This hexagonal

Manuscript received 31 March 2023; revised 17 July 2023; accepted 10 September 2023. Date of publication 17 November 2023; date of current version 13 November 2025. This work was supported by the National Natural Science Foundation of China under Grant 52377020. *(Corresponding author: Chi Zhang.)*

Li Ji and Fuchen Ge are with the College of Information Science and Engineering, China University of Petroleum-Beijing, Beijing 102249, China (e-mail: huanxir@126.com; 2021216007@student.cup.edu.cn).

Chi Zhang is with the Jiangsu Institute of Metrology (Jiangsu Energy Data Measurement Center), Nanjing 210023, China (e-mail: 2020211204@student.cup.edu.cn).

Color versions of one or more figures in this article are available at https://doi.org/10.1109/TPEL.2023.3319577.

Digital Object Identifier 10.1109/TPEL.2023.3319577

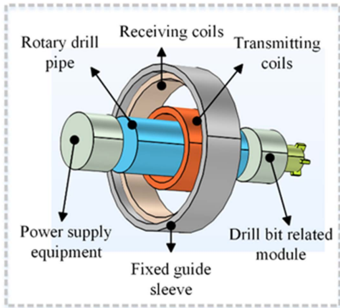

Fig. 1. Typical device for rotary steerable wireless power transmission.

structure design effectively improved the stability of transmission performance in the rotation process, but the structure was not equipped with protective shield, so the ferrite was more likely to be damaged in the rotation process.

Based on the above-mentioned research content, this article first verifies the operating characteristics of rotary steerable drilling, and on this basis defines the transmission characteristics of the wireless power transmission system. The model of DD-DD coils with good lateral antimigration performance was selected for design, and the influence law of the center angle of DD-type transmitting coils and the number of combinations on mutual inductance between transmitting and receiving coils were explored. In this article, the problem of mutual inductance zero coupling point in rotation process is analyzed, and a design scheme of double-layer orthogonal DD transmitting coils is proposed. Through the finite-element simulation design, the mutual inductance and antimigration characteristics in the rotation process are studied. The experimental model is built, and the transmission characteristics of the system are analyzed and summarized.

II. Rotation Condition and Circuit Analysis

A. Rotary Steerable Drilling Conditions

A typical device for rotary steerable wireless power transmission is shown in Fig. 1. It consists of a power supply module, a rotary drill pipe, a fixed guide sleeve, a wireless power transmission system, and a drill bit related module. The power module first supplies power to the transmitting coils located on the rotating drill pipe, and then transmits it to the receiving coils on the fixed guide sleeve using the principle of electromagnetic resonance. Finally, it supplies power to the relevant module of the bit through a series of power conversion circuits to ensure the stable and normal operation of the bit. During the drilling process, there will be relative rotation and relative migration motion between the drill pipe and the sleeve. The research focus of this article is to ensure the stability of coupling performance under moving conditions.

B. WPT Circuit Analysis

This section focuses on the power transmission characteristics under the S-S compensation topology. The equivalent circuit diagram of the WPT system based on the S-S compensation topology is shown in Fig. 2. In the designed DD-4D double-layer

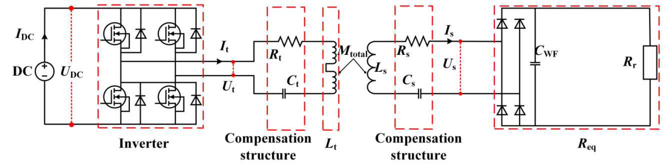

Fig. 2. Equivalent circuit diagram of WPT system based on S-S compensation topology.

orthogonal magnetic coupling structure, because the two transmitting coils are always orthogonal and in a mutual decoupling state, the cross-mutual inductance between them is defined as 0, and only the mutual inductance between the transmitting coil and the receiving coil is considered. In Fig. 2, the inner transmitting coil and the outer transmitting coil are equivalent to a transmitting coil loop L_{t} (equivalent self-inductance), and the S-S compensation topology is adopted to improve the power factor and reduce the energy loss. For convenience, it is assumed that the dc power supply, rectifier, and inverter used are ideal components. In Fig. 2, U_{dc} is the output voltage of the dc power supply, I_{dc} is the output current of the dc power supply, U_{t} is the output voltage of the inverter, I_{t} is the current of the equivalent transmitting loop, C_{t} and R_{t} represent the compensation capacitance and internal resistance of the equivalent transmitting coil, respectively. I_{s} is the receiving loop current, L_{s}, C_{s}, and R_{s} represent the self-inductance, compensation capacitance, and internal resistance of the receiving coil, respectively. U_{s} is the input voltage of the rectifier, C_{WF} is the filter capacitor, R_{r} is the load, M_{total} represents the total mutual inductance between the transmitting coil and the receiving coil, and R_{eq} is the equivalent load.

According to Kirchhoff's voltage theorem, (1) can be obtained, when $j\omega L_{\mathrm{t}}+1/j\omega C_{\mathrm{t}}=0$, $j\omega L_{\mathrm{s}}+1/j\omega C_{\mathrm{s}}=0$, the system resonance occurs. At this time, solving (1) can obtain (2) of I_{t} and I_{s}.

$$\begin{cases} U_{\mathrm{t}} = I_{\mathrm{t}}\left(j\omega L_{\mathrm{t}} + \frac{1}{jwC_{\mathrm{t}}} + R_{\mathrm{t}}\right) + jwM_{\text{total}}I_{\mathrm{s}} \\ 0 = I_{\mathrm{s}}\left(j\omega L_{\mathrm{s}} + \frac{1}{jwC_{\mathrm{s}}} + R_{\mathrm{s}}\right) + I_{\mathrm{s}}R_{\mathrm{eq}} + jwM_{\text{total}}I_{\mathrm{t}} \end{cases} \tag{1}$$

$$\begin{cases} I_{\mathrm{t}} = \frac{U_t(R_{\mathrm{s}}+R_{\mathrm{eq}})}{R_{\mathrm{t}}(R_{\mathrm{s}}+R_{\mathrm{eq}})+\omega^2 M_{\text{total}}^2} \\ I_{\mathrm{s}} = \frac{j\omega M_{\text{total}}U_t}{R_{\mathrm{t}}(R_{\mathrm{s}}+R_{\mathrm{eq}})+\omega^2 M_{\text{total}}^2} \end{cases}. \tag{2}$$

Assuming that the inverter and rectifier are ideal components, the output power P_{out} and transmission efficiency η of the WPT system based on the S-S compensation topology can be obtained

$$P_{\text{out}} = \frac{\omega^2 M_{\text{total}}^2 U_t^2 R_{\text{eq}}}{\left[R_{\mathrm{t}}\left(R_{\mathrm{s}}+R_{\text{eq}}\right)+\omega^2 M_{\text{total}}^2\right]^2} \tag{3}$$

$$\eta = \frac{\omega^2 M_{\text{total}}^2 R_{\text{eq}}}{\left(R_{\mathrm{s}}+R_{\text{eq}}\right)\left[R_{\mathrm{t}}\left(R_{\mathrm{s}}+R_{\text{eq}}\right)+\omega^2 M_{\text{total}}^2\right]}. \tag{4}$$

It can be seen from (4) that mutual inductance plays a major role in efficiency. Therefore, the mutual inductance characteristics of DD-DD coil structure with good lateral migration resistance will be studied in the following. Aiming at the problem of zero coupling point of mutual inductance, the DD-4D double-layer orthogonal magnetic coupling structure is proposed and its mutual inductance characteristics and antimigration characteristics are analyzed. The research flow chart

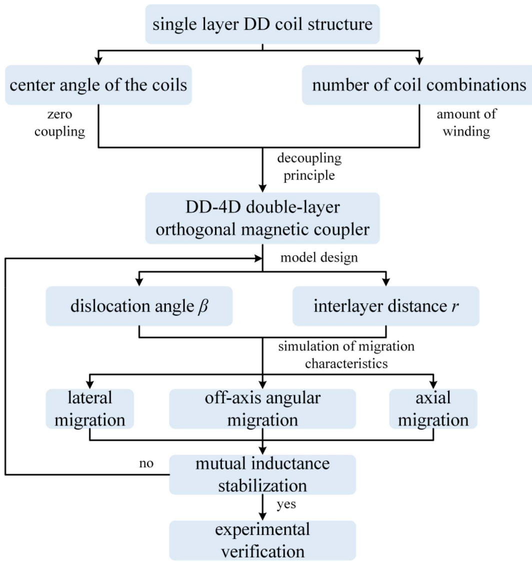

Fig. 3. Research content flow chart of DD-4D double-layer orthogonal magnetic coupling structure.

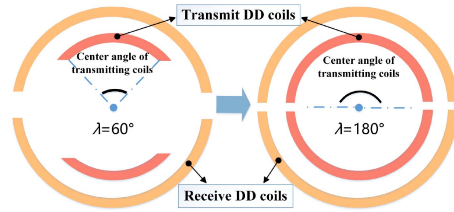

Fig. 4. Schematic diagram of the change of the center angle of the transmitting coils.

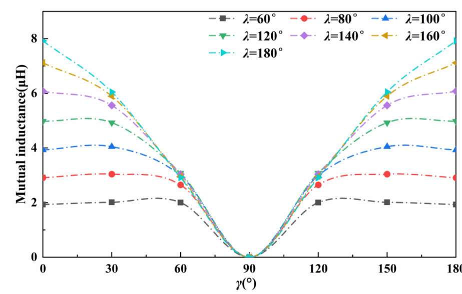

Fig. 5. Change trend of mutual inductance under different λ.

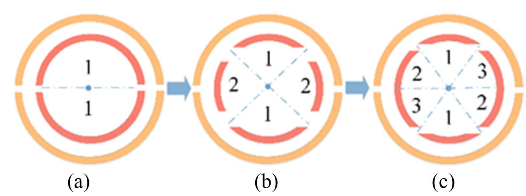

Fig. 6. Schematic diagram of the change of the group numbers of the transmitting coils. (a) Single coils. (b) Double coils. (c) Triple coils.

of DD-4D double-layer orthogonal magnetic coupling structure is shown in Fig. 3. First, the influence of different center angles of single-layer DD transmitting coils and the number of combinations on the mutual inductance of the coupled structure was investigated. Considering the requirements of stable mutual inductance, small winding amount of coils, and maximum average mutual inductance during rotation, a DD-4D double-layer orthogonal magnetic coupling structure was proposed based on the principle of coil decoupling. Second, the control variable method is used to simulate the misalignment angle and the distance between the two layers of transmitting coils, and the coil structure parameters with the best coupling performance are obtained. Finally, considering the inevitable strong vibration environment in the actual rotary steerable drilling conditions, the antimigration characteristics of the coupled structure are simulated and analyzed, and the DD-4D double-layer orthogonal coupled structure has superior antimigration performance under the conditions of lateral migration, axial migration, and off-axis angular migration, respectively.

III. Single-Layer DD Coil Model

In the planar coil model, DD coils have better antimigration performance, which is reflected in the DD coils having good lateral antimigration ability in rotation condition. Therefore, the three-dimensional DD-DD coil model was first selected as the design model in this article. The mutual inductance characteristics of the structure during rotation were analyzed and optimized, and the influences of the center angle of the transmitting coils and the number of coils combinations on the coupling performance were explored, respectively.

A. *Center Angle Analysis*

As shown in Fig. 4, the transmitting and receiving coils are placed facing each other, and the initial central angle of the transmitting coils is designed to be 60°. By changing the central angle λ of the transmitting coils, the finite-element simulation model is used to explore the mutual inductance characteristics in the rotation process of the magnetic coupler of DD-DD when λ ranges from 60° to 180°. The relative rotation angle of the transmitting and receiving coils is defined as γ, and when the transmitting and receiving coils are placed directly opposite as shown in Fig. 4, γ is 0. Fig. 5 is the mutual inductance change curve of magnetic coupler with different λ values in 180° rotation cycle. It is not difficult to find that although the magnetic coupler with smaller central angle λ changes more smoothly, but this is because the magnetic coupler with smaller value of λ in the rotation process of the overall mutual inductance smaller, and no matter how the value of the central angle λ changes. The mutual inductance values all approach zero at the position with a relative rotation angle of 90°, which is called the zero coupling point of mutual inductance.

In order to explore the influence of the number of transmitting coils combinations on the mutual inductance characteristics of the magnetic coupler in the rotation process, three transmitting coil combinations are designed, which are single-group transmitting DD model, double-group transmitting DD model and three-group transmitting DD model, as shown in Fig. 6. The central angle λ of these three models are about 180°, 90°, and 60°, respectively. The coil winding method that covers all the rotating drill pipe is realized.

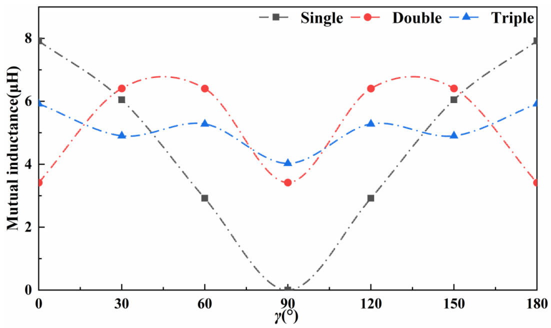

Fig. 7. Change trend of mutual inductance under different group numbers.

B. Combined Quantity Analysis of Coils

Fig. 7 shows the variation curve of mutual inductance of different transmitting coil combinations in the rotation process. It can be found that with the increase of the number of transmitting coil combinations, the fluctuation of mutual inductance curve becomes stable gradually. The two-group transmitting DD model increases the value of mutual inductance zero coupling point to 3.418 μH, while the three-group transmitting DD model increases it to 4.03 μH. The effect of zero coupling points of mutual inductance is weakened. However, compared with the dual-group emission DD model, the mutual inductance value at nonzero coupling points also decreases, and the coil winding quantity increases with the increase of the number of transmitting coil groups.

Through analysis and research, the reason for the existence of zero coupling point of mutual inductance is similar to the decoupling principle of DDQ coil [24]. The transverse magnetic field is generated at the central position of DD coil, and longitudinal magnetic field is generated at this position when the rectangular coil and DD coil are directly aligned. No coupling occurs between them, so the two kinds of coils are decoupled. Based on this design idea, in order to eliminate zero coupling points of mutual inductance and realize mutual inductance compensation, a new DD-4D double-layer orthogonal magnetic coupler is proposed in this article. While the receiving coils remain unchanged as DD model, the transmitting coils are designed as 4D double-layer orthogonal structure, and the structure is modeled and analyzed. The effects of the misalignment angle and interlayer distance parameters on the coupling performance were studied.

IV. DD-4D Double-Layer Coils Model

A. DD-4D Magnetic Coupler Modeling

Mutual inductance and coupling coefficient are important standards to measure the coupling state at the transceiver side. As the relative rotation angle between the transmitting and receiving coils changes, reducing the mutual inductance migration can improve the transmission efficiency stability of the coupling mechanism and reduce the power loss [25], [26], [27]. The DD-4D double-layer orthogonal magnetic coupler proposed in this article is composed of six subcoils, namely four transmitting coils and two receiving coils, as shown in Fig. 8. Fig. 8(a) shows the tiling diagram of the receiving coils. l_{31} represents the length

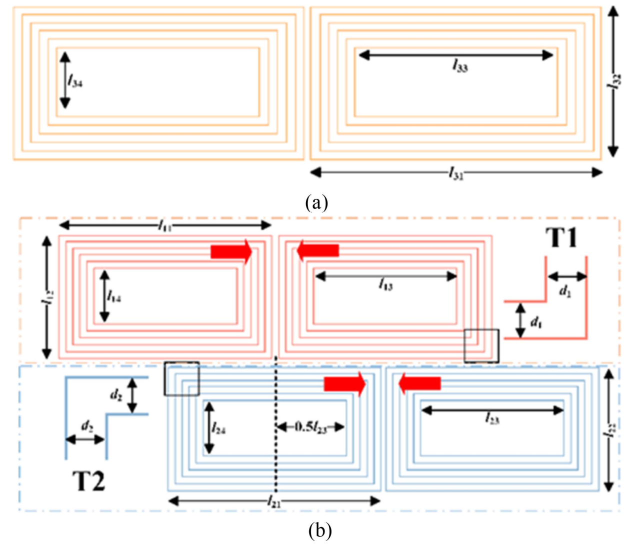

Fig. 8. Tile diagram of coils. (a) Receiving coils. (b) Transmitting coils.

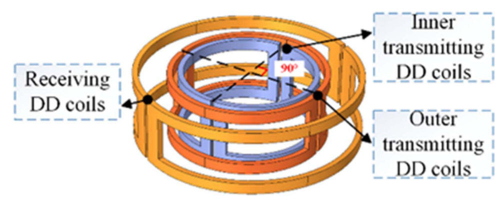

Fig. 9. DD-4D double-layer orthogonal magnetic coupler stereogram.

of the outermost receiving coils, and l_{32} represents the height of the outermost receiving coils. Fig. 8(b) shows the tiling diagram of the transmitting coils, which consists of two groups of DD coils, T_1 and T_2. l_{11} and l_{21} represent the outermost coil lengths of the two groups of transmitting coils, respectively, l_{12} and l_{22} represent the height of the outermost coil, and d_1 and d_2 represent the distance between turns of the coils.

Fig. 9 is a stereogram of DD-4D double-layer orthogonal magnetic coupler. The transmitting side is composed of two sets of DD coils with a tangential difference of 90°, which are tightly wound around the outer surface of the rotating drill pipe. The receiving side is a single group of DD coils, which are tightly wound on the inner surface of the fixed guide sleeve and coaxial with the transmitting coils. Limited by the outer diameter of the rotating shaft, the diameter of the two transmitting coils are 150 mm and 154 mm, respectively, and the diameter of the receiving coils is 200 mm due to the inner diameter of the sleeve. According to the coil model determined earlier, the influence of misalignment angle between double-layer coils and interlayer distance parameters on the coupling performance of the system was studied.

B. Optimization Analysis of Coil Dislocation Angle

In order to illustrate the necessity of orthogonalization of double-layer transmitting coils in the proposed DD-4D magnetic coupler, the dislocation angle β between double-layer transmitting coils is simulated in this section, and the influence of different β values on mutual inductance of the magnetic coupler

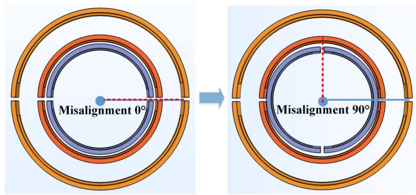

Fig. 10. Schematic diagram of the misalignment angle of the transmitting coils.

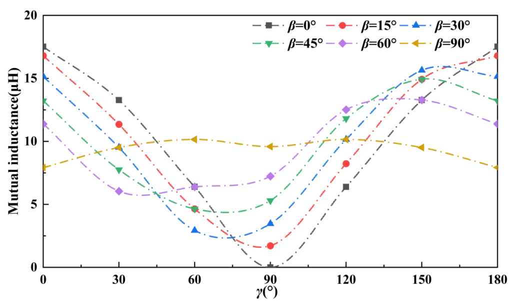

Fig. 11. Change trend of mutual inductance under different misalignment angles.

in the rotation process is explored. Keep the parameters of receiving coils fixed, and only change β value in simulation. Fig. 10 is a schematic diagram of coils dislocation angle. When the dislocation is 0°, the two layers of transmitting coils are aligned, and when the dislocation is 90°, the two layers of transmitting coils are orthogonal. Fig. 11 shows the variation curve of mutual inductance M of the magnetic coupler during the process of γ from 0° to 180° at different β angles. It can be found that when $\beta = 0°$, the mutual inductance value at $\gamma = 90°$ is close to 0, because the two layers of transmitting coils position are right, did not play the role of compensating mutual inductance. When the β value is increased, the minimum mutual inductance increases. It is clearly observed that compared with the other five curves in the figure, the $\beta = 90°$ curve fluctuates smoothly, the mutual inductance migration is only 21.9%, and the M is maintained at about 9 μH during the rotation period, which successfully solves the problem of zero coupling point of mutual inductance. It is proved that the orthogonalization of double-layer transmitting coils in DD-4D magnetic coupler is correct, so the double-layer orthogonal transmitting coils model is selected for further study.

C. Optimization Analysis of Interlayer Distance Between Loops

The change of the interlayer distance r will also affect the coupling performance of the system. The relationship between the interlayer distance r and the rotational mutual inductance M of the magnetic coupler will be simulated and analyzed in the following. Keep other parameters of the transceiver coils unchanged, and only change the value of r. Fig. 12 shows the relationship between mutual inductance M of the DD-4D double-layer orthogonal magnetic coupler, rotation angle γ, and interlayer distance r. The size of the inner transmitting coil is fixed, and the interlayer distance r is increased from 2 to 10 mm, and it is found that the average mutual inductance increases

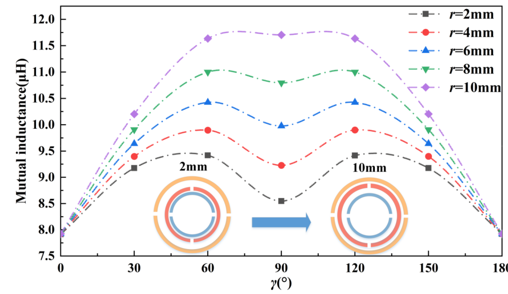

Fig. 12. Variation trend of mutual inductance at different interlayer distances.

TABLE I
PARAMETERS OF DOUBLE-LAYER QUADRATURE DD COIL

Outer transmitting coil		Inner transmitting coil		Receiving coil	
l_{11}	233.5 mm	l_{21}	251.2 mm	l_{31}	314 mm
l_{12}	90 mm	l_{22}	90 mm	l_{32}	90 mm
l_{13}	195.5 mm	l_{23}	211.2 mm	l_{33}	274 mm
l_{14}	50 mm	l_{24}	50 mm	l_{34}	50 mm

within the rotation cycle. This is because the larger the r value is, the closer the distance between the outer transmitting coil and the receiving coil is, the more magnetic inductance lines will be absorbed, resulting in the increase of mutual inductance M. It can be seen from the figure that with the increase of the interlayer distance, the mutual inductance fluctuation near the original zero coupling point gradually weakens. When the interlayer distance r is 10 mm, the mutual inductance of the transceiver coil is almost unchanged within the rotation range of 60° to 90°. However, in the complete rotation process, the fluctuation trend of mutual inductance M gradually becomes stronger, and the mutual inductance migration rate increases from 15.94% at $r = 2$ mm to 32.31% at $r = 10$ mm. In addition, from the perspective of practical application, when the interlayer distance is too large, the outer transmitting coil is actually in the middle position between the fixed sleeve and the rotating drill pipe. Lacking the means of fixation and susceptible to environmental influences, the transmitting coil should be fixed as close to the rotating drill pipe as possible for the stability of the equipment. To sum up, double-layer orthogonal DD coils with the dislocation of inner and outer layers of 90° and the distance between layers of 2 mm were finally selected for further study.

V. Simulation Analysis of Migration Characteristics

Due to the limitation of practical application conditions, the geometric parameters of coil model are fixed as shown in Table I, and the number of turns is designed to be 6. Based on the periodic characteristics of rotational motion, only the process of rotation angle from 0° to 180° needs to be analyzed. In order to verify that the double-layer orthogonal magnetic coupler has good antioffset performance in the rotation process, the characteristics of lateral offset and axial offset of the coil model are simulated and analyzed in the following.

A. Lateral Migration

The geometric parameters of the fixed coils are unchanged, the number of turns is 6, and the spacing of turns is 2 mm. The

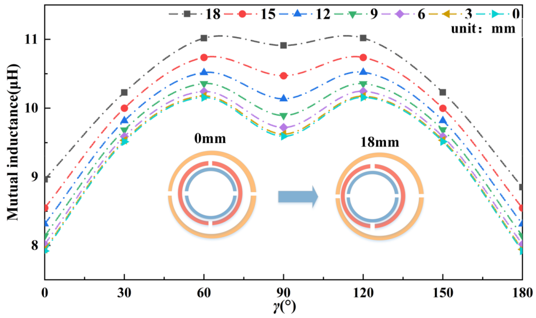

Fig. 13. Changes in mutual inductance with lateral migration.

migration disturbance of the receiving and transmitting coils is simulated in actual working conditions. Due to the limitation of the size parameters of the rotating drill pipe and the fixed guide sleeve, the maximum lateral migration is 20 mm. The changes in mutual inductance of the magnetic coupler of the transmitting coil from the zero's migration position to the lateral migration position of 18 mm will be explored in the following. Fig. 13 shows the variation law of rotational mutual inductance of the transmitting coil at different migration positions. Since the magnetic coupler is presented as a three-dimensional circle, the lateral migration of the transmitting coil on both sides has exactly the same influence. For the convenience of analysis, only the migration in Fig. 13 is considered. As can be seen from the figure, mutual inductance presents an overall upward trend with the increase of lateral migration, and the curve becomes more stable when γ is in the range of 60° to 150° near the position of decoupling between the receiving coil and the inner transmitting DD coils. The main reason is that the transmitting coil is close to the receiving coil at this position, and the coupling magnetic flux increases when the outer transmitting coil and the receiving coil are directly opposite, and the growth rate is greater than the magnetic flux reduced by the other side away from the receiving coil. Therefore, when transverse migration occurs, the coupling performance of the local region of the double-layer DD coil model is improved, and the mutual inductance migration rate changes little within the complete rotation cycle. When the maximum migration is 18 mm, the mutual inductance migration rate is only 19.6%, and the mutual inductance fluctuation is reduced by 2.4% compared with the zero migration position, and the overall mutual inductance variation range is smaller. It is proved that the coil model can maintain the stability of system transmission when lateral migration occurs.

B. Axial Migration

Since the height of the transmitting coil is designed to be 90 mm, the range of axial migration is considered from 0 to 80 mm when simulating the transmitting coil axial migration disturbance. Fig. 14 shows the variation law of rotational mutual inductance of transmitting coils at different migration positions when the transmitting and receiving coils are axially migration. It can be seen from Fig. 14 that, with the increase of axial migration, mutual inductance on the whole presents a downward trend and the coupling performance becomes weaker. This is because the axial migration distance between the transmitting

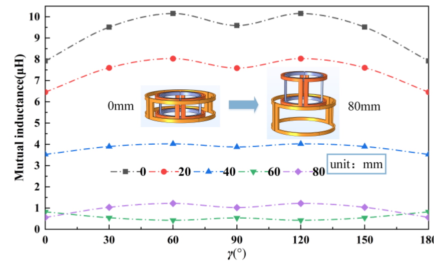

Fig. 14. Changes in mutual inductance with axial migration.

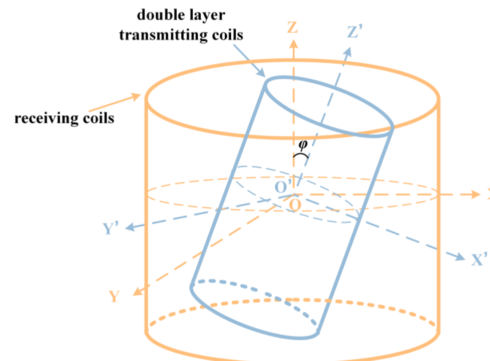

Fig. 15. Diagram of off-axis angular migration of coupled structure.

coil and the receiving coil is too large, and only a small part of the magnetic inductance line generated is coupled to the receiving coil, making the mutual inductance value M smaller. When the migration is larger than 60 mm, that is, two-thirds of the coil height, mutual inductance is greatly reduced and fluctuates greatly, making it almost difficult to achieve effective power transmission. When the axial migration is 20 and 40 mm, the mutual inductance migration rate is 20% and 12.3%, which is better than 22% under the zero migration condition. Therefore, the double-layer orthogonal magnetic coupler of DD-4D can ensure the effective transmission of electric energy when the axial migration is less than 40 mm.

C. Off-Axis Angular Migration

In downhole rotary steerable drilling conditions, off-axis angular migration is easy to occur when rotating drill pipe and fixed guide sleeve work, which affects the work of the WPT system. Fig. 15 shows the schematic diagram of off-axis angular migration of the coupling structure, where φ is the off-axis angle between the transmitting coil and the receiving coil. The effect of off-axis angular migration of the transmitting coil in the X' and Y' directions is exactly the same, and only the migration in Fig. 15 is considered for ease of analysis. Due to the limitation of coil parameters in Table I, the maximum φ migration is set to 30°. Fig. 16 shows the variation law of rotational mutual inductance of the transmitting coil under different φ migration conditions.

It is not difficult to find that with the increase of φ value, the average mutual inductance during rotation shows a downward trend, and the coupling performance weakens. This is because the off-axis angle is too large, only a small part of the magnetic inductance line generated by the transmitting coil is coupled to the receiving coil, so that M is reduced. In the range of $\varphi = 0°$ to

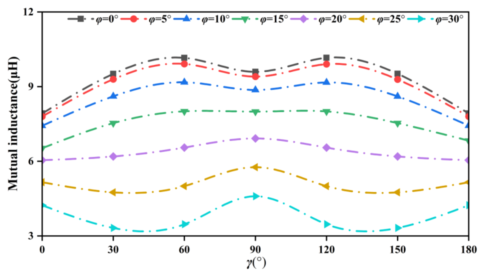

Fig. 16. Changes in mutual inductance with off-axis angular migration.

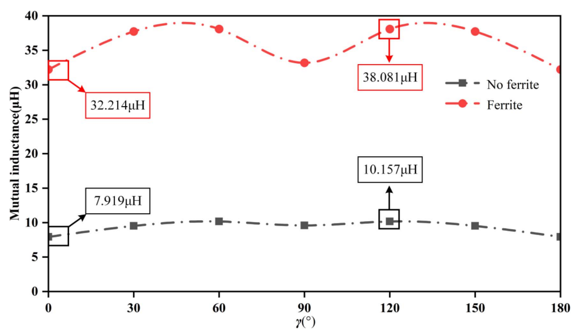

Fig. 17. Variation of mutual inductance with rotation angle in the presence of ferrite.

$\varphi = 20°$, the migration rate of mutual inductance decreases from 22% to 14.4%, and the stability is improved. In the range of $\varphi = 20°$ to $\varphi = 30°$, the mutual induction migration rate increases from 14.4% to 38%, which affects the normal operation of the system. However, according to the actual underground work, it can be seen that the migration value φ of the coupling structure is very small, far less than 20°. Therefore, the DD-4D double-layer orthogonal magnetic coupling structure can ensure the effective transmission of electric energy when the migration angle is less than 20°.

D. Ferrite Simulation

Due to the DD-4D double-layer orthogonal magnetic coupling structure, the mutual inductance value only has a maximum variation of 22% during the rotation period. Considering the role of ferrite material in dredge the magnetic inductance line, in order to minimize the mutual inductance change of the coupled structure, ferrite is added to the DD-4D double-layer orthogonal magnetic coupling structure. Fig. 17 shows the simulation diagram of the mutual inductance value changing with the rotation angle in the presence of ferrite. In the actual application conditions in the oil downhole, considering the strong vibration environment in the well and the friability problem of ferrite, the fully closed covering method is adopted to lay it inside the transmitting coil and outside the receiving coil, respectively. According to the data in the figure, it is not difficult to find that the average mutual inductance value of the DD-4D double-layer orthogonal magnetic coupling structure during the 180° rotation period is greatly improved after adding ferrite. From 8 μH without ferrite to 35 μH, the mutual inductance change rate also decreased from 22% to 18.2%, a decrease of 3.8%. In terms of antimigration performance, Table II shows the mutual

TABLE II
MUTUAL INDUCTANCE OF COUPLED STRUCTURAL MIGRATION

	No ferrite	Ferrite
Lateral migration	7.919 µH(0 mm)	32.214 µH(0 mm)
	8.965 µH(18 mm)	36.334 µH(18 mm)
Axial migration	7.919 µH(0 mm)	32.214 µH(0 mm)
	3.526 µH(40 mm)	17.768 µH(40 mm)
Off-axis angular migration	7.919 µH(0°)	32.214 µH(0°)
	4.233 µH(30°)	21.133 µH(30°)

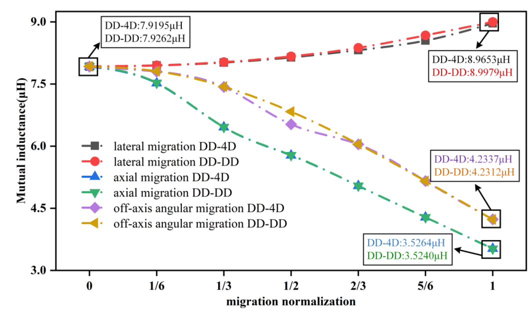

Fig. 18. Comparison diagram of mutual inductance between two coil structures in the case of migration.

inductance values of coupled structure migration in the presence of ferrite. According to Table II, in the conditions of lateral migration, axial migration, and off-axis angular migration, the mutual inductance migration rate after adding ferrite to the coupled structure is reduced by 0.38%, 10.63%, and 12.15%, respectively, which effectively proves that adding ferrite can not only minimize mutual inductance change, but also minimize mutual inductance change. At the same time, the antimigration performance of DD-4D double-layer orthogonal magnetic coupling structure can be enhanced to some extent.

E. Antimigration Performance Comparison

The mutual inductance values of DD-4D double-layer orthogonal magnetic coupling structure remain relatively stable during 180° rotation period, which is obviously better than that of single-layer DD-DD structure. In order to verify the antimigration performance of the DD-4D double-layer orthogonal magnetic coupling structure, mutual inductance is compared with that of the single-layer DD-DD structure from three angles of lateral migration, axial migration, and off-axis angular migration. According to the previous research content, the migration values of lateral migration, axial migration, and off-axis angular migration are normalized. Fig. 18 shows the mutual inductance comparison diagram of DD-4D double-layer orthogonal magnetic coupling structure and single-layer DD-DD structure under three kinds of migration conditions. It is not difficult to find from the data in the figure that in the lateral migration, the coupling structure proposed in this article reduces the mutual inductance migration rate from 13.5% of DD-DD to 13.1%. In axial migration, the DD-4D double-layer orthogonal magnetic coupling structure reduces the mutual inductance migration rate from 55.5% to 55.4%. In off-axis angular migration, the coupling structure proposed in this article reduces the mutual inductance

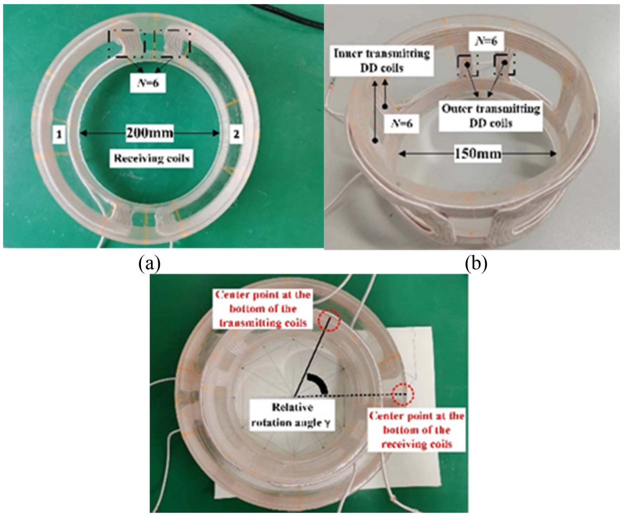

Fig. 19. Physical picture of transmitting and receiving coils. (a) DD receiving coils. (b) Double-layer orthogonal transmitting coils. (c) Double-layer orthogonal magnetic coupler.

TABLE III
MODEL PARAMETER

Description	Symbol	Value
Double layer orthogonal transmitting coils self-induction	L_t	47.618 μH
Receiving coils self-induction	L_s	26.575 μH
Double layer orthogonal transmitting coils compensates capacitance	C_t	87 nF
Receiving coils compensation capacitance	C_s	132 nF
Frequency	f	85 kHz

migration from 46.6% of DD-DD to 46.5%. Compared with axial migration and off-axis angular migration, lateral migration has better resistance characteristics, which effectively verifies that the antimigration performance of DD-4D double-layer orthogonal magnetic coupling structure is better than that of single-layer DD-DD structure under three migration conditions, and is more suitable for application in rotary steerable drilling conditions.

VI. Experimental Verification and Analysis

In order to verify the stability of mutual inductance parameters and transmission efficiency of the DD-4D double-layer orthogonal magnetic coupler in the rotation process, an experimental platform based on the structure was built in this section. First, the LCR instrument was used to measure the variation law of mutual inductance and coupling coefficient of the transmitting and receiving coils in the rotation process. Then a complete WPT system was built, and the transmission efficiency was recorded and analyzed by using S-S resonance compensation network structure. The actual transmitting and receiving coils created are shown in Fig. 19. The number of turns of both transmitting and receiving coils is six turns, and the turns spacing d_1 and d_2 are 2 mm. Winding is carried out according to the coil parameter data in Tables I and III shows the self-inductance

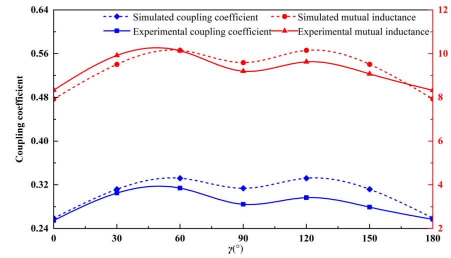

Fig. 20. Variation of mutual inductance and coupling coefficient with rotation angle.

value, compensation capacitance value, and frequency of the transmitting and receiving coils.

The relationship between mutual inductance, coupling coefficient, and rotation angle γ of DD-4D double-layer orthogonal magnetic coupler was obtained through experiments and simulation, as shown in Fig. 20. It can be seen that rotation angle is closely related to mutual inductance, and when the transmitting coil rotates 180°, mutual inductance and coupling coefficient fluctuate by one cycle. It can also be seen that in the simulation curve, the mutual induction of DD-4D double-layer orthogonal magnetic coupler reaches the minimum value of 7.9 μH when $\gamma = 0°$ and 180°, and the maximum value of 10.1 μH when $\gamma = 60°$ and 120°. Although the overall variation trend of mutual inductance and coupling coefficient is similar between the experimental curve and the simulation curve, there is still some migration in the data results, which is mainly reflected in the error of mutual inductance is about 4.1% and the error of coupling coefficient is 9.2% when $\gamma = 90°$. When $\gamma = 120°$, the error of mutual inductance is about 5.1% and the error of coupling coefficient is 10.6%. The main reason for the migration is that the experimental coil winding is not accurate enough and there is inevitable operating error.

The change curve of mutual inductance and coupling coefficient between DD-4D double-layer orthogonal magnetic coupler and independent outer layer DD or independent inner layer DD model in the rotation process is shown in Fig. 21. It is not difficult to find that the average mutual inductance value of outer DD coil in the rotation cycle is slightly larger than that of inner DD coil, because its radius size is larger and its distance from the receiving coil is relatively close. The magnetic lines coupled to are more density, so the mutual inductance value is slightly larger. It can also be found that in the process of relative rotation of the transmitting and receiving coil of 360°, there are two zero coupling points separated by 180°, whether the outer DD coil or the inner DD coil is used alone, and the DD-4D double-layer orthogonal magnetic coupler can achieve compensation for the zero coupling point, so that the coupling coefficient and mutual inductance can remain relatively stable. The coupling coefficient k is kept above 0.25, and the mutual inductance coefficient M is kept above 8 μH.

The DD-4D double-layer orthogonal magnetic coupling structure designed in this article is applied to the rotary steerable drilling conditions in oil downhole. Fig. 22 shows the physical structure diagram of the rotary steerable wireless power transmission system. The rotary steerable drilling tool is composed

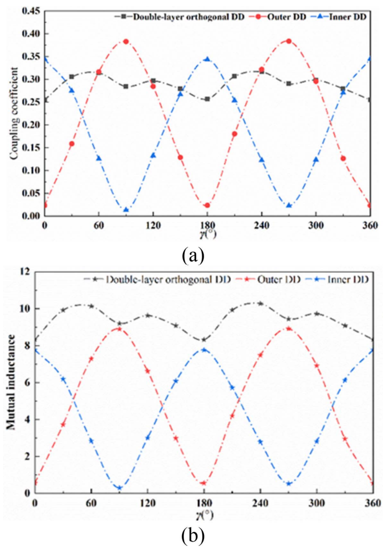

Fig. 21. Changes in coupling coefficients and mutual inductance during rotation. (a) Coupling coefficient. (b) Mutual inductance.

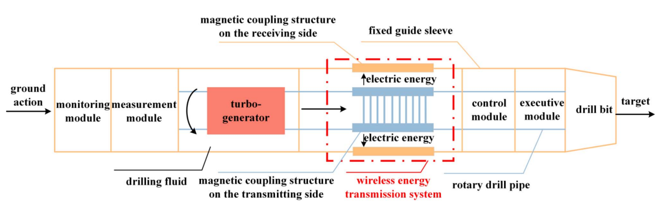

Fig. 22. Schematic diagram of the physical structure of a rotary steerable wireless energy transmission system.

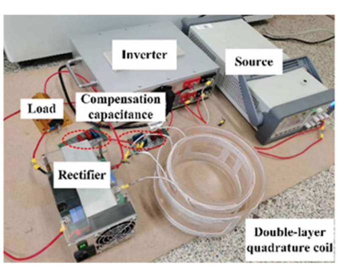

Fig. 23. WPT system experiment platform.

of fixed guide sleeve, rotary drill pipe, drill bit, and so on. The rotary drill pipe is connected to the downhole turbine generator, and the drilling fluid is between the rotary drill pipe and the fixed guide sleeve. The migration of the drill bit and the guiding function are driven by the electric energy transferred between the rotary drill pipe and the fixed guide sleeve. The focus of the work in this article is to transmit energy to the receiving coil wound inside the fixed guide sleeve through the transmitting coil wound outside the rotating drill pipe, and then provide power to the executive module on the sleeve. The overall WPT system, as shown in Fig. 23, is composed of power supply, inverter, compensation capacitor, DD-4D double-layer orthogonal coil, rectifier, and load. The inverter is used to generate square wave voltage, and the rectifier is used to obtain stable output.

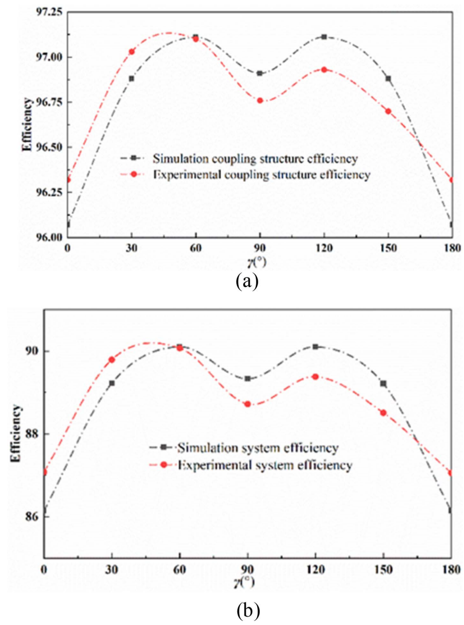

Fig. 24. Variation of transmission efficiency with rotation angle. (a) Transmission efficiency of magnetic coupler. (b) System transmission efficiency.

In the overall system experiment, the variation of the magnetic coupler efficiency and the system efficiency with the relative rotation angle of the transmitting and receiving coils are shown in Fig. 24. The variation trend of the transmission efficiency of the simulation and experiment is consistent. When the multiple of $\gamma = 90°$, there is a local minimum, that is, the zero coupling point of the original DD-DD coil model. It can be seen that the double-layer orthogonal DD coil model effectively compensates the transmission efficiency at the zero coupling point. In the whole rotation process, the maximum transmission efficiency of the magnetic coupler can reach 97.03%, the minimum transmission efficiency is 96.32%, and the efficiency migration is only 0.732%. The maximum efficiency of the system is 90.07%, the minimum is 87.06%, and the migration rate is only 3.34%. The curve of the simulation results is symmetric about $\gamma = 90°$, and because the coil cannot be wound accurately in the experiment, there is inevitable operating error, so the curve of the experimental results is asymmetric, when the rotation angle is less than 90° experimental efficiency is higher than the simulation efficiency, the rotation angle is greater than 90° is vice versa.

VII. Conclusion

In the field of wireless power transmission, rotary wireless power transmission technology has been paid more and more attention. In this article, a novel DD-4D double-layer orthogonal magnetic coupler is proposed, and the mutual inductance difference between it and DD-DD magnetic coupler is investigated. In this article, the mutual inductance and lateral and axial antimigration characteristics of the proposed DD-4D double-layer orthogonal magnetic coupler during rotation are analyzed. The experimental model of WPT has been constructed and tested.

The experimental results are in good agreement with the simulation results. During the rotation period, the mutual inductance is maintained around 8 μH, and the maximum error is about 5.1%. The transmission efficiency of the system reaches 90.07% and the migration rate is only 3.34%, which effectively verifies the validity of the DD-4D double-layer orthogonal magnetic coupler.

References

[1] L. Kirschbaum, D. Roman, G. Singh, J. Bruns, V. Robu, and D. Flynn, "AI-driven maintenance support for downhole tools and electronics operated in dynamic drilling environments," *IEEE Access*, vol. 8, pp. 78683–78701, 2020.

[2] M. Gonzalez, H. R. Seren, G. Ham, E. Buzi, G. Bernero, and M. Deffenbaugh, "Viscosity and density measurements using mechanical oscillators in oil and gas applications," *IEEE Trans. Instrum. Meas.*, vol. 67, no. 4, pp. 804–810, Apr. 2018.

[3] F. Florence, "Upstream oil and gas drilling processes and instrumentation open to new technology," *IEEE Instrum. Meas. Mag.*, vol. 16, no. 6, pp. 6–10, Dec. 2013.

[4] A. B. Nassif, "Assessing the impact of harmonics and interharmonics of top and mudpump variable frequency drives in drilling rigs," *IEEE Trans. Ind. Appl.*, vol. 55, no. 6, pp. 5574–5583, Nov./Dec. 2019.

[5] C. Gan, W.-H. Cao, L.-Z. Wang, K.-Z. Liu, and M. Wu, "An improved dynamic optimization control system for the drilling rate of penetration (ROP) and its industrial application," *IEEE Trans. Ind. Electron.*, vol. 70, no. 6, pp. 6201–6208, Jun. 2023.

[6] J. Zhang, W. Lan, C. Deng, F. Wei, and X. Luo, "Thermal optimization of high-temperature downhole electronic devices," *IEEE Trans. Compon., Packag., Manuf. Technol.*, vol. 11, no. 11, pp. 1816–1823, Nov. 2021.

[7] A. Albert, O. M. Aamo, J.-M. Godhavn, and A. Pavlov, "Suppressing pressure oscillations in offshore drilling: Control design and experimental results," *IEEE Trans. Control Syst. Technol.*, vol. 23, no. 2, pp. 813–819, Mar. 2015.

[8] O. J. Hoffmann, J. R. Jain, R. W. Spencer, and N. Makkar, "Drilling dynamics measurements at the drill bit to address today's challenges," in *Proc. IEEE Int. Instrum. Meas. Technol. Conf.*, 2012, pp. 443–448.

[9] A. Jinasena, G. O. Kaasa, and R. Sharma, "Improved real-time estimation of return flow rate of drilling fluids by model adaptation for friction parameter," *IEEE Sens. J.*, vol. 19, no. 20, pp. 9314–9323, Oct. 2019.

[10] F. Liu, Z. Ding, X. Fu, and R. M. Kennel, "Parametric optimization of a three-phase MCR WPT system with cylinder-shaped coils oriented by soft-switching range and stable output power," *IEEE Trans. Power Electron.*, vol. 35, no. 1, pp. 1036–1044, Jan. 2020.

[11] X. Zhang, F. Liu, and T. Mei, "Multifrequency phase-shifted control for multiphase multiload MCR WPT system to achieve targeted power distribution and high misalignment tolerance," *IEEE Trans. Power Electron.*, vol. 36, no. 1, pp. 991–1003, Jan. 2021.

[12] C. D. Rouse, S. R. Cove, Y. Salami, P. Arsenault, and A. Bartlett, "Three-phase resonant capacitive power transfer for rotary applications," *IEEE J. Emerg. Sel. Topics Power Electron.*, vol. 10, no. 1, pp. 160–169, Feb. 2022.

[13] R. Trevisan and A. Costanzo, "A 1-kW contactless energy transfer system based on a rotary transformer for sealing rollers," *IEEE Trans. Ind. Electron.*, vol. 61, no. 11, pp. 6337–6345, Nov. 2014.

[14] Z. Dai and J. Wang, "A dual-frequency WPT based on multilayer self-decoupled compact coil and dual CLCL hybrid compensation topology," *IEEE Trans. Power Electron.*, vol. 37, no. 11, pp. 13955–13965, Nov. 2022.

[15] P. Tan, T. Peng, X. Gao, and B. Zhang, "Flexible combination and switching control for robust wireless power transfer system with hexagonal array coil," *IEEE Trans. Power Electron.*, vol. 36, no. 4, pp. 3868–3882, Apr. 2021.

[16] Z. H. Ye, Y. Sun, X. Dai, C.-S. Tang, Z.-H. Wang, and Y.-G. Su, "Energy efficiency analysis of U-coil wireless power transfer system," *IEEE Trans. Power Electron.*, vol. 31, no. 7, pp. 4809–4817, Jul. 2016.

[17] X. Liu, X. Song, and X. Yuan, "Compensation optimization of the relay coil in a strong coupled coaxial three-coil wireless power transfer system," *IEEE Trans. Power Electron.*, vol. 37, no. 4, pp. 4890–4902, Apr. 2022.

[18] D. W. Seo, "Design method of three-coil WPT system based on critical coupling conditions," *IEEE J. Emerg. Sel. Topics Power Electron.*, vol. 9, no. 3, pp. 3802–3811, Jun. 2021.

[19] K. Song et al., "A rotation-lightweight wireless power transfer system for solar wing driving," *IEEE Trans. Power Electron.*, vol. 34, no. 9, pp. 8816–8830, Sep. 2019.

[20] A. Abdolkhani, A. P. Hu, and N. K. C. Nair, "A double stator through-hole type contactless slipring for rotary wireless power transfer applications," *IEEE Trans. Energy. Convers.*, vol. 29, no. 2, pp. 426–434, Jun. 2014.

[21] L. Wang, J. Li, H. Chen, and Z. Pan, "Radial-flux rotational wireless power transfer system with rotor state identification," *IEEE Trans. Power Electron.*, vol. 37, no. 5, pp. 6206–6216, May 2022.

[22] Z. Yan, B. Song, Y. Zhang, K. Zhang, Z. Mao, and Y. Hu, "A rotation-free wireless power transfer system with stable output power and efficiency for autonomous underwater vehicles," *IEEE Trans. Power Electron.*, vol. 34, no. 5, pp. 4005–4008, May 2019.

[23] A. Abdolkhani, A. P. Hu, G. A. Covic, and M. Moridnejad, "Contactless slipring system based on rotating magnetic field principle for rotary applications," in *Proc. IEEE Energy Convers. Congr. Expo.*, 2013, pp. 2566–2573.

[24] A. Ahmad, M. S. Alam, and A. A. S. Mohamed, "Design and interoperability analysis of quadruple pad structure for electric vehicle wireless charging application," *IEEE Trans. Transp. Electrific.*, vol. 5, no. 4, pp. 934–945, Dec. 2019.

[25] Z. Zhang, H. L. Pang, A. Georgiadis, and C. Cecati, "Wireless power transfer-an overview," *IEEE Trans. Ind. Electron.*, vol. 66, no. 2, pp. 1044–1058, Feb. 2019.

[26] S. Liu, J. Su, J. Lai, J. Zhang, and H. Xu, "Precise modeling of mutual inductance for planar spiral coils in wireless power transfer and its application," *IEEE Trans. Power Electron.*, vol. 36, no. 9, pp. 9876–9885, Sep. 2021.

[27] K. Zhang, Y. Ma, Z. Yan, Z. Di, B. Song, and A. P. Hu, "Eddy current loss and detuning effect of seawater on wireless power transfer," *IEEE J. Emerg. Sel. Topics Power Electron.*, vol. 8, no. 1, pp. 909–917, Mar. 2020.

Li Ji received the Ph.D. degree in power electronics and power drives from the Institute of Electrical Engineering, Chinese Academy of Sciences, Beijing, China, in 2018.

She is currently with the College of Information Science and Engineering, China University of Petroleum-Beijing, Beijing, China. Her research interests include wireless power transfer system, energy internet, and simultaneous transmission of wireless power and information.

Fuchen Ge received the B.E. degree in information engineering in 2021 from the China University of Petroleum-Beijing, Beijing, China, where he is currently working toward the M.S. degree with the Institute of Information Engineering.

His research interests include the composition network technology of the wireless power transfer system and the energy internet.

Chi Zhang received the M.S. degree in engineering from China University of Petroleum-Beijing, Beijing, China, in 2023.

He is currently with the Jiangsu Institute of Metrology (Jiangsu Energy Data Measurement Center), Nanjing, China. His research interests include the optimization of magnetic coupling mechanism and electromagnetic compatibility testing.